Hamerton, I., Tang, W., Anguita, J. V., & Silva, S. R. P. (2015). Dramatic reductions in water uptake observed in novel POSS nanocomposites based on anhydride-cured epoxy matrix resins. *Materials Today Communications*, *4*, 186-198. https://doi.org/10.1016/j.mtcomm.2015.07.001

Dramatic reductions in water uptake observed in novel POSS nanocomposites based on anhydride-cured epoxy matrix resins

Ian Hamerton[1,*], Winnie Tang,[2] Jose V. Anguita,[2] and S. Ravi P. Silva[2]

[1]The Advanced Composites Centre for Innovation and Science, Department of Aerospace Engineering, University of Bristol, Queen's Building, University Walk, Bristol, BS8 1TR, United Kingdom.

[2]Advanced Technology Institute, Faculty of Engineering and Physical Sciences, University of Surrey, Guildford, Surrey, GU2 7XH, United Kingdom.

Correspondence to: I. Hamerton (E-mail: ian.hamerton@bristol.ac.uk)

ABSTRACT

A methylnadic anhydride-cured diglycidylether of bisphenol A, is prepared and characterised and a mono-epoxy POSS reagent added (0.5-4 wt-%) to produce a series of nanocomposites. Two reaction mechanisms are observed involving esterification at lower temperatures (60-180 °C) and etherification at temperatures above 180 °C. Using the Ozawa and Kissinger methods, the activation energy for the first reaction was found to be 87-90 kJ/mol and 122-124 kJ/mol for the second reaction. Incorporation of POSS into the epoxy-anhydride network increases the T_g and cross-link density, indicating a more rigid network, but the values do not follow a trend based solely on POSS content. The char yield increases with POSS content with very little change in the degradation temperature. Incorporation of POSS (1 wt-%) can reduce the moisture uptake in the cured resin by ~25 % at 75 % relative humidity. This is accompanied by a lower impact on glass transition temperature: the T_g is reduced by 10 K at saturation, compared with 31 K for the unmodified epoxy.

Key words: Epoxy resins, nanocomposites, POSS, water uptake.

1. Introduction

Epoxy resins are one of the most important families of cross-linked, thermosetting polymers [1], which offer a good balance of desirable properties in the neat resin when: flexural strength (100-140 MPa), tensile strength (45-60 MPa), compressive strength (130 MPa) and impact strength (G_{IC} = 100-125 J/m^2) coupled with a reasonably high glass transition temperature (T_g) of 130-165 °C, depending on postcure [2]. This has led their widespread use in a variety of applications, including advanced composites, adhesives and as high performance dielectrics for

microelectronic applications (typical dielectric constants are between 3-4 and dissipation factors of 0.002 to 0.020 under ambient conditions). Polymerization may occur either in the absence or in the presence of curing agents, and in this particular instance an anhydride is employed. The cured epoxy also displays good adhesion to a variety of substrates, hardness, chemical inertness and thermal resistance, but the effect of the size of the polymer network (*i.e.* the conversion) on the final properties can be highly significant. Thus, it is important to be able to predict the likely changes in properties in order that cure conditions might be optimised and in a previous paper [3] we reported the use of molecular simulation to predict both glass transition temperatures and thermal stability in diamine-cured epoxy resins as the cure parameters are varied.

However, the propensity of epoxy resins to absorb moisture, due to the generation of a hydroxyl group with every ring-opening reaction, is an acknowledged drawback associated with their use in applications in which retention of mechanical properties in hot/wet conditions is key. The epoxy system studied here is space qualified for use in structural composites in satellite applications and thus already displays a comparatively low moisture uptake in the unmodified state. However, as the construction of a larger satellite may take a number of months (even years) to complete, then even thicker structures may reach equilibrium moisture content during this timescale. Once sorbed, this moisture will tend to remain within the matrix until it is deployed in an extra-terrestrial environment, when the dramatic reduction in atmospheric pressure serves to cause the molecular water to be removed (violently in some instances) from the composite, potentially leading to delamination or small vibrations in rigid boom structures, which can disturb the operation of optical benches.

Polyhedral oligomeric silsesquioxanes (or POSS reagents) are well known [4] for the benefits in thermal and mechanical properties that they can confer when incorporated into both thermoplastic [5] and thermoset [6] polymers. The dimensions of the silica polyhedral are such that the materials may be covalently bound (a variety of functional groups can be introduced at the vertices) and compatible at the molecular scale. One of the aims of this work is to explore the influence of POSS on reducing moisture uptake in an anhydride-cured epoxy resin based on the diglycidyl ether of bisphenol A (DGEBA), preferably whilst retaining or improving other desirable physical and mechanical properties.

2. Experimental

2.1 Materials

The epoxy oligomer, based on DGEBA (Araldite LY556, eew = 175.5 ± 3.5 g/mol., Haas Group International), methylnadic anhydride (HY906, Haas Group International) and methylimidazole accelerator (DY070, Sigma Aldrich) (Scheme 1) were characterised using Raman and ^{1}H NMR

spectroscopy and used as received. Epoxycyclohexylisobutyl POSS (EP0402) was obtained from Hybrid Plastics, Inc. and used as received.

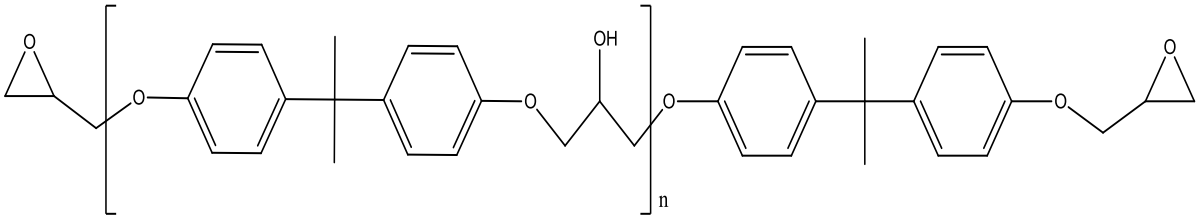

Araldite LY556 (DGEBA)

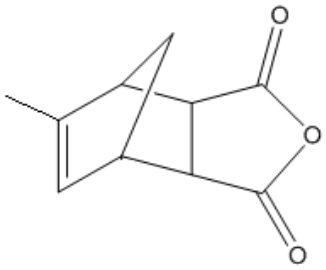

HY906
(methylnadic anhydride)

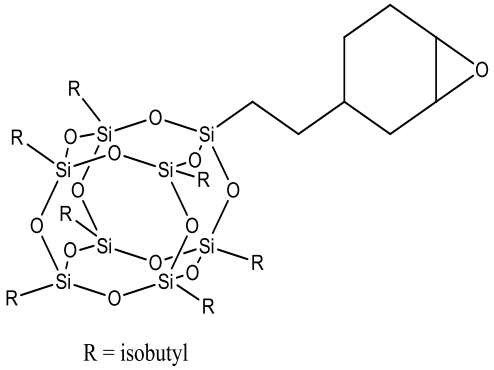

EP0402
(epoxycyclohexylisobutyl POSS)

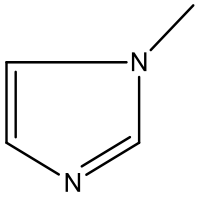

DY070
(methylimidazole)

Scheme 1. Structures of the reagents used in this work.

2.2 Vibrational spectroscopy

Spectra were obtained using a Perkin-Elmer system 2000 FT-NIR-Raman spectrometer operating at 250 mW (Nd-YAG laser) and a Perkin-Elmer FTIR system 2000 spectrometer. Samples were analysed *in situ* during the cure process using Raman spectroscopy employed a heated cell that was ramped rapidly from room temperature to 60°C and held isothermally for 4 hours; spectra being taken at intervals of 7.5 minutes. For each measurement, 16 spectra were obtained at a resolution of 4 cm^{-1} and co-added to produce the final spectrum. Samples were post cured at 130°C (3 hours). Chemometrics analysis (PCA) was carried out on the spectral data using The Unscrambler X, v10.1 software (Camo, Oslo).

2.3 Differential scanning calorimetry (DSC)

DSC was undertaken using a TA Instruments Q1000 running TA Q Series Advantage software on samples (6.0 ± 0.5 mg) in hermetically sealed aluminium pans. Dynamic experiments were conducted at a heating rate of 10 K/min. from room temperature to 250 °C (heat/cool/heat)

under flowing nitrogen (50 cm^3/min.). For isothermal analyses samples were heated at 50 K/min. to 60, 70, 80, 90, 100, 110 and 120 °C and held at the final temperature for 1- 3 hours, then cooled to room temperature at 10 K/min. The T_g was determined from the midpoint of the inflexion in the heat flow curve during both the cooling step and the re-scan (heating) experiment.

2.4 Blending and cure of polymer samples for thermo-mechanical analyses

The mono-epoxy POSS (EP0402) (various quantities were studied at 0.5, 1, 2, and 4 wt-% or 5.2 x 10^{-5} – 4.2 x 10^{-4} mol.) was dissolved in a minimum quantity of tetrahydrofuran (THF) followed by addition of the methyl nadic anhydride (4.75 g, 5.8 x 10^{-2} mol.) and the methylimidazole (0.08 g, 9.78 x 10^{-4} mol.). The mixture was stirred at 80 °C on a heating plate (2 hours or until full dissolution had occurred). Pre-reaction was conducted to ensure that the POSS was more readily dispersed within first the curing agent and then more easily combined/distributed within the epoxy. The resulting mixture was then placed into a vacuum oven at 50 °C (1 hour) to ensure that all the solvent had been removed. DGEBA (5 g, 2.8 x 10^{-2} mol., based on EEW = 175.5 g/mol.) was then added to the mixture and stirred (5-10 minutes) until a homogeneous mixture was formed. The final compositions along with sample designations are shown in Table 1.

Table 1 Composition of the blends studied in this work

Sample	**Blend component g (mol.)**			
	DGEBA (LY556)	**M□□□□□□□□□□□□□□□□□□□□ (HY906)**	**□□□□□□□□□□□□□□□□□□□□ (DY070)**	**POSS (EP0402)**
1	5 (2.8 x 10^{-2})	4.75 (5.8 x 10^{-2})	0.08 (9.78 x 10^{-4})	-
2				4.9 x 10^{-2} (5.2 x 10^{-5})
3				9.8 x 10^{-2} (1.0 x 10^{-4})
4				1.96 x 10^{-1} (2.1 x 10^{-4})

5				3.92×10^{-1} (4.2×10^{-4})

The resulting samples were then cooled and stored (refrigerated) prior to analysis. Samples for DMTA measurements were cured in aluminium dishes (55 mm diameter, depth 10 mm) in a fan-assisted oven: heating from room temperature to 60°C (4 hours isothermal) + heating to 130°C (3 hours isothermal) followed by a gradual cool to room temperature. Cured samples were cut to the correct token size for analysis using a diamond saw.

2.5 Dynamic mechanical thermal analysis (DMTA)

DMTA was carried out in single cantilever mode at a frequency of 1 Hz on cured neat resin samples (2 mm x 15 mm x 35 mm) using a TA Instruments Q800 operating in static air.

2.6 Thermogravimetric analysis (TGA)

Thermogravimetric analysis (TGA) was performed on a TA Instruments Q500 on cured particulate resin samples (7.5 ± 0.5 mg) in a platinum crucible from 20-800°C at 10 K/min in nitrogen (40 cm^3/min).

2.7 Moisture Uptake

For the determination of moisture content, samples of cured epoxy nanocomposites (2 mm x 12 mm x 30 mm) ±0.5 mm were conditioned in three chambers each of controlled relative humidity: 33 % RH (containing magnesium chloride), 53 % RH (containing magnesium nitrate) and 75 % RH (containing sodium chloride); each salt solution comprised distilled water. Samples were allowed to equilibrate over approximately 12 months and the moisture content of the cured epoxy resins was determined periodically by wiping excess moisture from the surface with a tissue and measuring the increase in mass.

3. Results and Discussion

3.1 Spectral analysis of the uncured blends

The reaction mechanism between an anhydride curing agent and epoxy resin is complex, for at least three competing reactions can take place: the reaction between the anhydride with the hydroxyl groups on the epoxy oligomer to form half-esters; the reaction of the half-ester with an epoxide ring generating another hydroxyl; and the newly formed hydroxyl reacting with another anhydride, or in the presence of free acid, it can react with another epoxy to form an ester

linkage [7]. Imidazoles are generally used to initiate the epoxy anhydride reaction and to accelerate the cure (Scheme 2). Prior to cure, the blends and their individual components were initially characterised using a variety of spectral techniques to monitor the reaction of the blend in the absence of the POSS reagent and the FTIR spectra of the individual components (DGEBA, methyl nadic anhydride and the methylimidazole accelerator). There is a slight decrease in band intensity at ~917 cm^{-1} for the cured resin compared to the DGEBA oligomer. This band can be assigned to the epoxy group, which during the process of curing undergoes ring opening and lends to a reduction in intensity. The ester carbonyl band at ~1730 cm^{-1} (C=O stretch) shows that the reaction between the anhydride and epoxy has taken place forming ester linkages. The disappearance of the asymmetric and symmetric carbonyl stretches in the final cured structure at 1780 cm^{-1} and 1850 cm^{-1} respectively also confirms that the reaction between the anhydride and epoxy has taken place. In this process the anhydride reacts with a hydroxyl group to form an ester link and a carboxylic acid. The carboxylic acid formed in the first step reacts with an epoxide ring. Upon ring opening, the hydroxyl can react with another anhydride or with an oxirane ring. Lewis acids or bases can be used to accelerate the cure reaction. In this instance, the methylimidazole acts as a Lewis base and acts as an accelerator for the anhydride/epoxy reaction activate the anhydride and produce a carboxylate anion that can open the epoxy ring. Scheme 2 shows the accepted reaction mechanism of the methyl nadic anhydride curing agent with an epoxy [8]. The imidazole produces adducts containing highly reactive alkoxide ions to initiate rapid anionic copolymerisation, *i.e.* esterification, between epoxies and anhydride. An excess of epoxy in the blend (as is the case in these blends, see Table 1) may also cause homo-polymerisation, *i.e.* etherification, of the epoxide groups, to some extent.

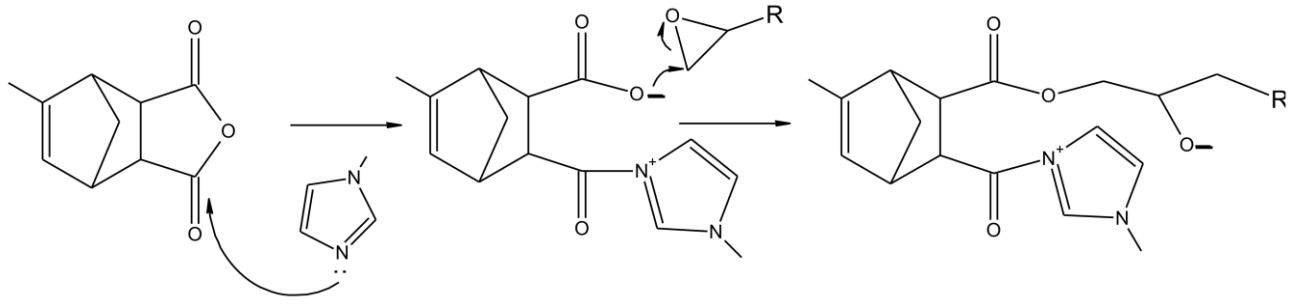

Scheme 2. Base catalysed anhydride/epoxy reaction

The FTIR spectrum of epoxycyclohexylisobutyl POSS (EP0402) exhibits a strong absorption band at 1085 cm^{-1} assigned to the asymmetric stretching vibration of Si-O-Si groups from the inorganic cage (Fig. 1, top).

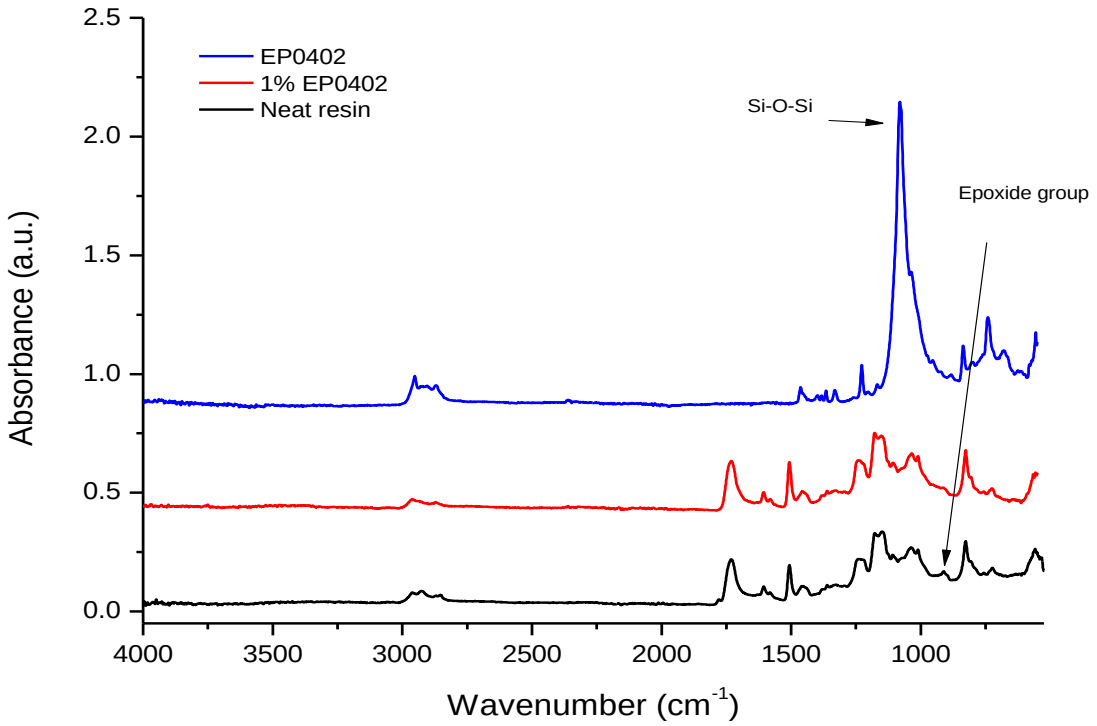

Fig. 1. FTIR spectra of EP0402 (top), sample **3** containing 1 wt-% EP0402 (middle) and sample **1**, neat epoxy-anhydride resin (bottom)

When EP0402 is added to the resin system, this band should still be present as the cage does not participate directly in the polymerisation reaction. The epoxy band at 920 cm^{-1} is of low intensity in the spectrum (Fig. 1, bottom) as the POSS is monofunctional and added in relatively low concentrations within this study. In the blend (Fig. 1, middle), the Si-O-Si band is difficult to discern due to the low quantity being added. Raman spectroscopy was used in a complementary fashion to FTIR spectroscopy. During the curing reaction of the unmodified blend (in the absence of POSS), the asymmetric and symmetric stretches of the epoxy ring at 920 cm^{-1} and 866 cm^{-1} respectively decrease in intensity, due to the consumption of the epoxy groups. The concentration of anhydride rings, which decrease during the reaction, can be assigned to the asymmetric and symmetric carbonyl stretches at 1850 cm^{-1} and 1780 cm^{-1} respectively. During the curing reaction between anhydride and epoxy groups the rapid formation of ester groups occurs and this is reflected in the presence of new bands at 1730 cm^{-1} and 2970 cm^{-1}; the latter corresponds to the asymmetric stretch of the CH_2 group adjacent to the ester group (Fig. 2).

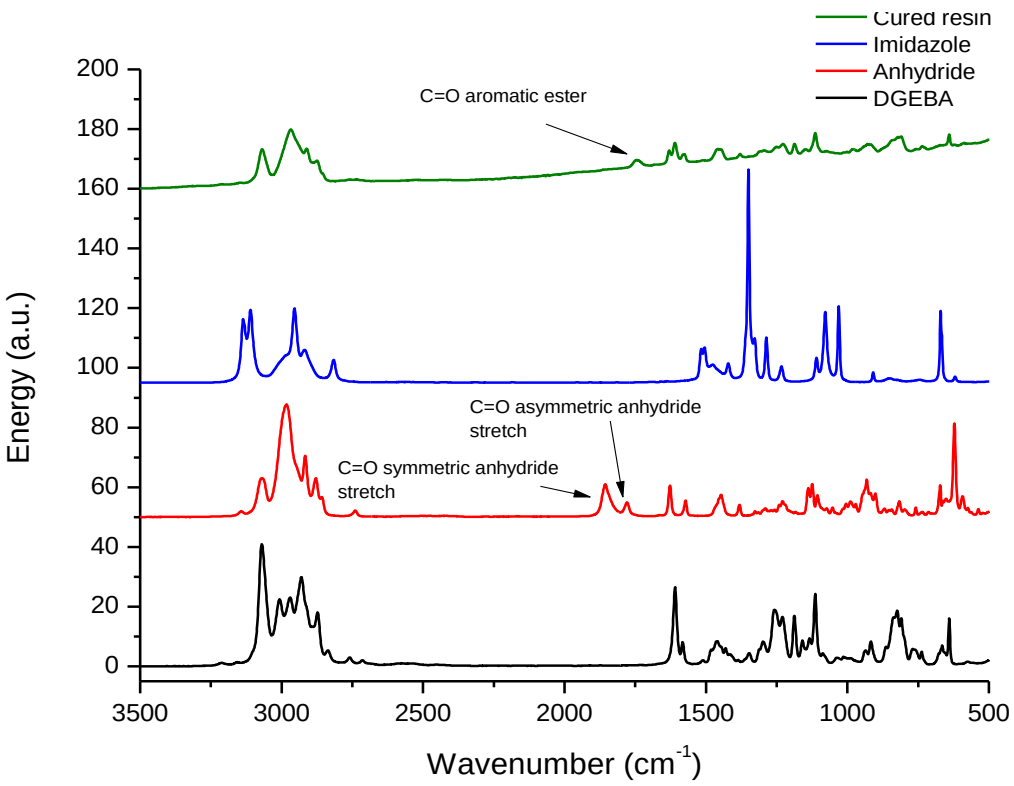

Fig. 2. Raman spectra of the sample **3** containing 1 wt-% EP0402 (top), imidazole (top middle), anhydride (bottom middle) and DGEBA epoxy (bottom)

After post-curing the initially flat baseline becomes increasingly steep as the sample becomes fluorescent, as a consequence of the formation of conjugated structures within the polymer network. This is observed in the final cured resin resulting in poorly resolved vibrations at lower wavenumber. The Raman spectrum of the mono-epoxy POSS (EP0402) shows several sharp bands, due mainly to the aliphatic moieties; the asymmetric stretching of CH_3 at 2955 cm^{-1}, asymmetric stretching of CH_2 at 2928 cm^{-1} and the symmetric stretching of CH_2 at 2870 cm^{-1}. The Si-C stretching is also visible at 1331 cm^{-1}.

3.2 Isothermal analysis of the polymerisation of the epoxy-anhydride blend using DSC

Initially, the polymerisation of the unmodified blend was analysed using isothermal DSC to provide baseline data against which the nanocomposites might be compared. At the start of the reaction, the cure rate is dominated by the reactivity of the monomers before being controlled by the diffusion phenomena as the viscosity increases. Fig. 3 (top) shows the rate of reaction *vs.* time for the epoxy-anhydride blend. As the temperature increases so does the rate of reaction. It is also clear that at isothermal temperatures between 100 and 130°C, the shapes of the curves are not symmetrical and some are distinctly bimodal, confirming that more than one reaction is taking place. Having determined through a rescan experiment that the DSC curves accounted for the full exotherm (with negligible residual exotherms evident on rescan), linear baselines were

applied and the exothermic peaks were integrated to determine the enthalpy of polymerisation (ΔH_p) and fractional conversion (α). When reaction conversion (making no attempt to de-convolute the different thermal events) is plotted as a function of reaction time for different curing temperatures between 80°C and 150°C (Fig. 3, bottom) there is a clear dependence on the reaction rate and cure temperature. As expected, at the start of the reaction, the cure rate is dominated by the reactivity of the monomers before being controlled by diffusion phenomena as the viscosity increases.

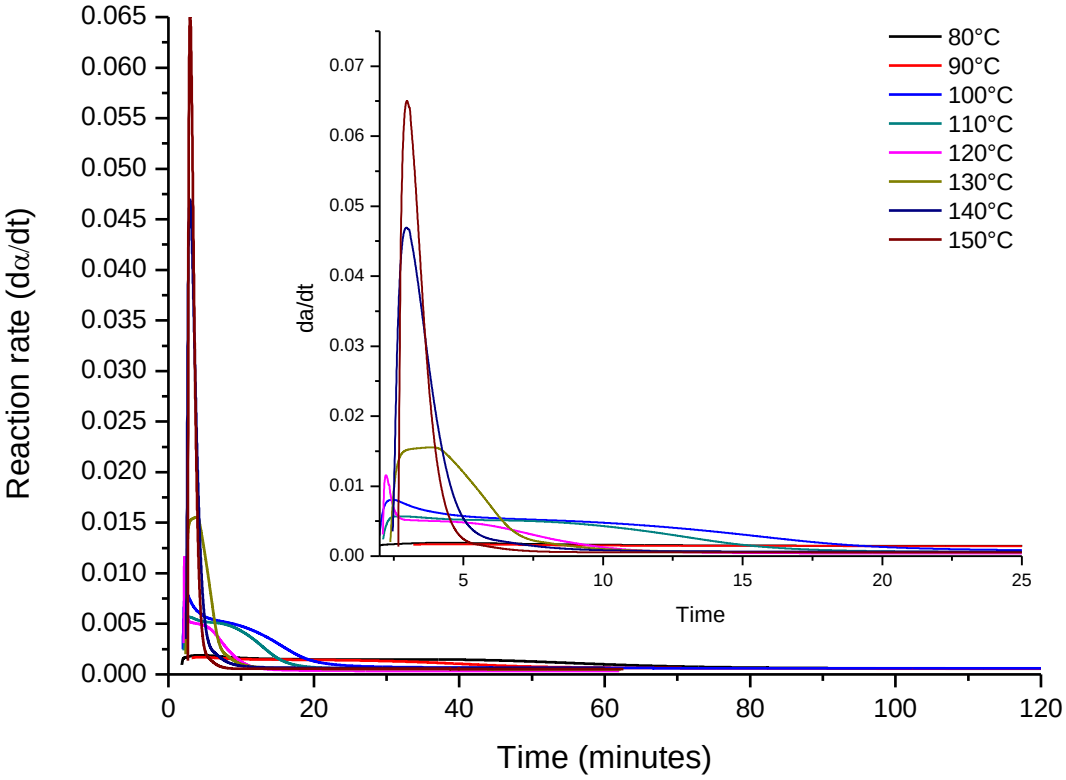

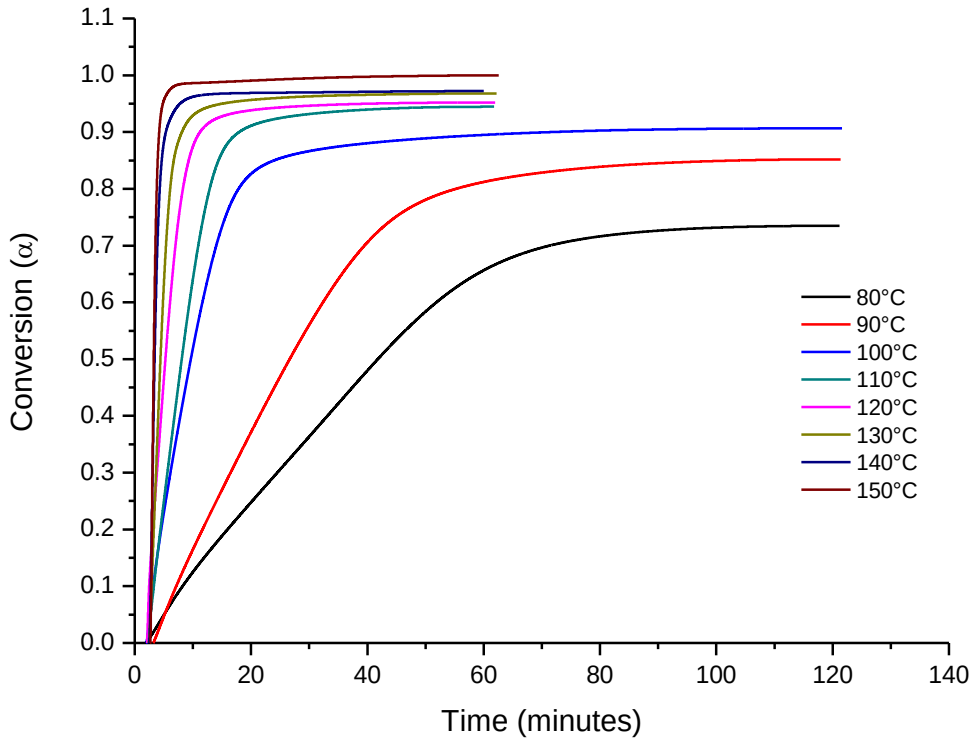

Fig. 3. Rate of reaction *vs.* time (top) and total conversion *vs.* time (bottom) at various isothermal temperatures of epoxy-anhydride blend (sample **1**). *N.B.* expansion 0-25 minutes shown inset.

Applying a phenomenological approach to the kinetic analysis of the DSC data, previously discussed in detail by Barton [9], the reaction rate may be given by the following general expression [10]:

$$d\alpha/dt = kf(\alpha) \qquad \text{(Eq. 1)}$$

where dα/dt is the reaction rate, $f(\alpha)$ is the differential conversion function and k is the temperature dependent reaction rate constant. The curing reaction can be described by a rate equation, which relates the rate of the reaction to the rate constant and the consumption of reactants or production of products. An Arrhenius relationship is typically used for the temperature dependent function and thus:

$$d\alpha/dt = \left(Ae^{-Ea/RT}\right)f(\alpha) \qquad \text{(Eq. 2)}$$

where A is the pre-exponential factor, E_a is the apparent activation energy, R is the ideal gas constant and T is the absolute temperature in Kelvin.

The *n*th order and autocatalytic kinetics are the two most commonly used reaction mechanisms that describe isothermal cure. In the case of thermoset curing, a generalized rate function utilizing the degree of cure, α, which is the disappearance of epoxide functional groups or

appearance of chemical bonds, with (1 - α) representing the epoxide group concentration. The *n*th order equation can expressed as following:

$$d\alpha/dt = k\ (1 - \alpha)^n \quad \text{(Eq. 3)}$$

However, many thermosetting materials (*e.g.* epoxy resins) are autocatalytic, so that the product of the reaction serves as an additional catalyst in the reaction.

Kinetic modelling of autocatalytic reactions requires an additional term to account for this effect, namely

$$d\alpha/dt = k\ \alpha^m(1 - \alpha)^n \quad \text{(Eq. 4)}$$

where α^m represents the catalytic effect of the products of the reaction with an order of *m*. Most epoxies exhibit either *n*th order or autocatalytic curing reactions, although it is not always apparent which type an epoxy will follow. However, the two types are readily differentiated by experimental data. As can be easily predicted from Equation 2, an *n*th order reaction will exhibit its maximum rate at the beginning of the reaction, whereas the autocatalytic reaction, predicted from Equation 3, will exhibit its maximum rate at some later time during the reaction. The reaction order is generally determined by plotting the degree of conversion as a function of time and fitting the curve. In addition to the time dependence of the rate of conversion, the rate constant, *k*, is temperature dependent, usually assumed to follow an Arrhenius relation of the form:

$$k = Ae^{-Ea/RT} \quad \text{(Eq. 5)}$$

where *k* is the reaction rate constant, *A* is the pre-exponential function, and E_a is the activation energy. Thus, Equations 2 and 3 can be rewritten as

$$d\alpha/dt = \left(Ae^{-Ea/RT}\right)(1 - \alpha)^n \quad \text{(Eq. 6)}$$

$$d\alpha/dt = \left(Ae^{-Ea/RT}\right)\alpha^m\,(1 - \alpha)^n \quad \text{(Eq. 7)}$$

with the incorporation of the Arrhenius temperature dependence. The initial rate of an autocatalytic reaction is not necessarily zero since the reaction can proceed *via* alternative paths, especially in the (likely) presence of impurities like water and catalyzing ions. Taking this into account, the autocatalytic equation developed by Sourer and Kamal [10] is given as

$$d\alpha/dt = (k_1 + k_2\,\alpha^m)\,(1 - \alpha)^n \quad \text{(Eq. 8)}$$

where k_1 and k_2 are the Arrhenius rate constants.

This treatment of the isothermal DSC data leads to the Arrhenius parameters shown in Table 1 for the epoxy-anhydride cure reaction. According to Horie *et al.*, E_{a1} is the activation energy of the reaction catalysed by proton donors initially present in the system [11]. E_{a2} is the activation energy for the reaction catalysed by proton donors, which are produced during curing. The reaction orders, *m* and *n*, were approximately 0.60 – 0.95 and 1.33 - 1.96 respectively. With increasing temperature, the apparent rate coefficients k_1 and k_2 increase, the hallmark of an autocatalytic reaction.

Table 2

Kinetic parameters of epoxy-anhydride resins from isothermal DSC analysis.

Temperature (°C)	**Activation energy (kJ/mol)**		**Pre-exponential factor (s^{-1})**		**Rate constant (s^{-1})**		**Rate order**		**Overall order**
	Ea₁	***Ea₂***	***A₁***	***A₂***	***k₁***	***k₂***	***m***	***n***	***m + n***
80	50.72	128.87	4.44×10^5	1.00×10^{17}	0.056	0.126	0.60	1.33	1.93
90					0.058	0.192	0.66	1.40	2.06
100					0.058	0.330	0.76	1.82	2.58
110					0.060	0.312	0.85	1.83	2.68
120					0.065	0.570	0.80	1.96	2.76
130					0.121	1.968	0.92	1.78	2.70
140					0.211	6.948	0.83	1.92	2.75
150					0.218	10.63	0.95	1.95	2.90

This temperature dependence of the Arrhenius relationship (Eq. 5) for the rate constants k_1 and k_2 is graphically shown in Fig. 4 from which two distinct regions in the data are evident, equating to a change in reaction mechanism. The curing mechanism of the epoxy-anhydride system is known to be complex (Scheme 3) and $\ln k_1$ and $\ln k_2$ appear to be best fitted with two separate linear plots.

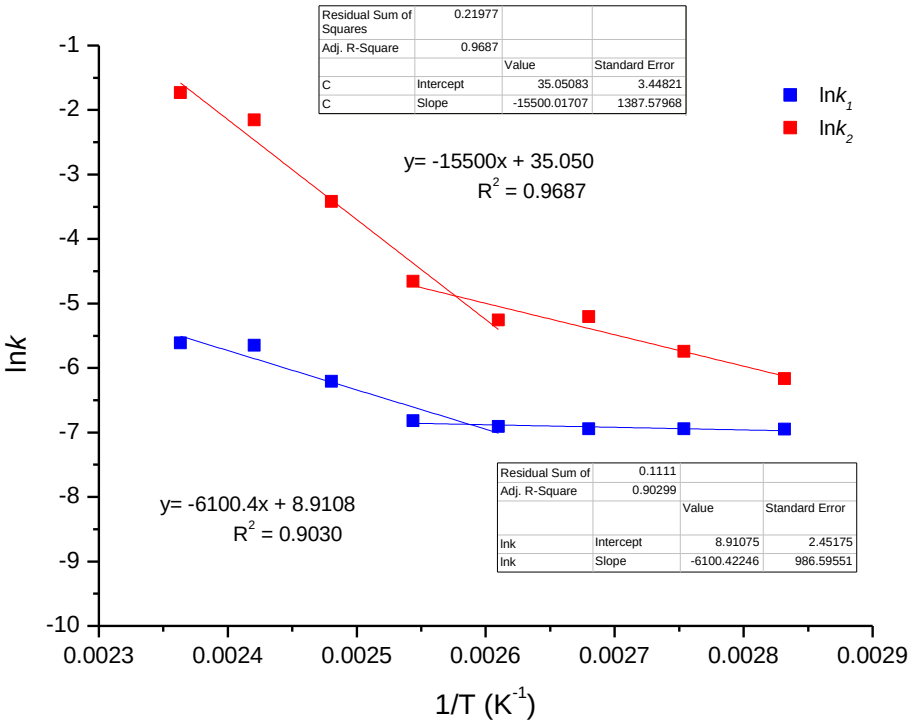

Fig. 4. Arrhenius-type plot for rate constant of epoxy-anhydride cure reaction.

At lower temperatures the imidazole can catalyse the anhydride forming an active complex (Scheme 3a). At the higher temperatures, the presence of –OH groups on the epoxy oligomers can also cause ring opening of the anhydride through proton transfer (Scheme 3b). The initiation and propagation of the polymerisation of epoxides by the imidazole can also take place (Scheme 3c).

(a)

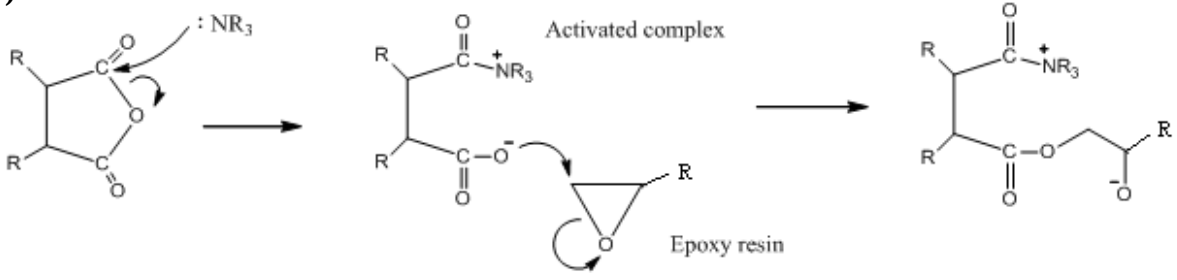

where NR_3 = 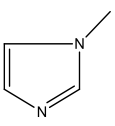

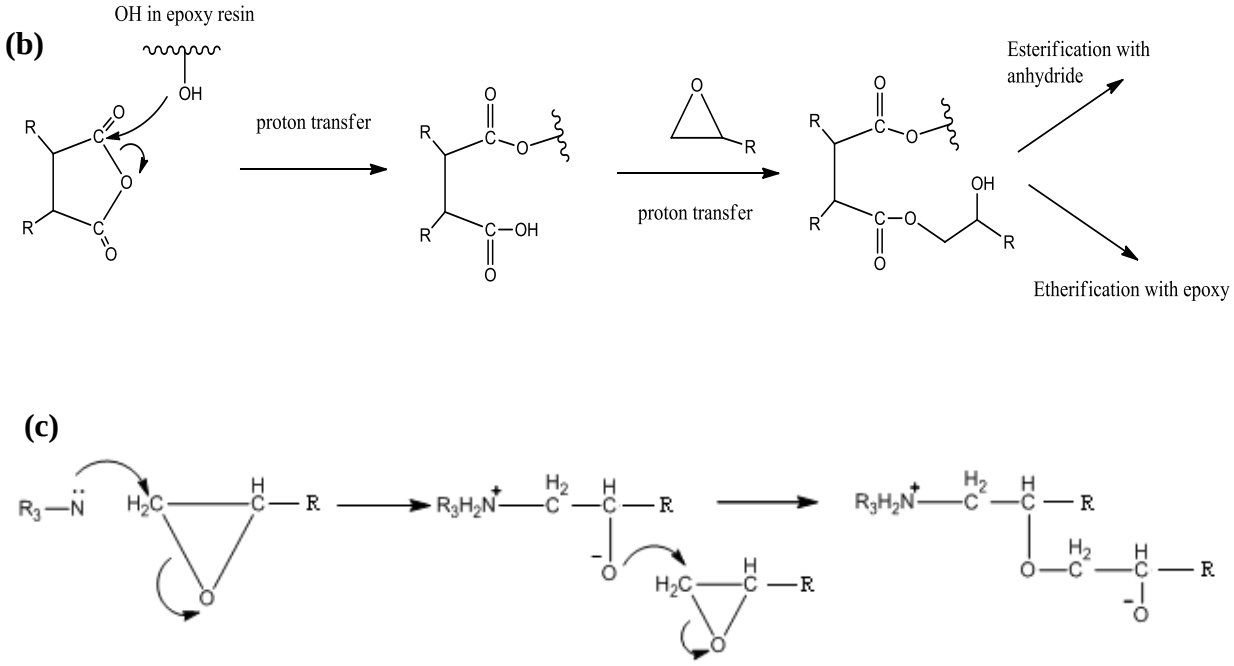

Scheme 3. Competing reaction mechanisms for an epoxy/anhydride/imidazole system: **(a)** base catalysed anhydride/epoxy reaction **(b)** uncatalysed anhydride/epoxy reaction and **(c)** base catalysed epoxy ring opening reaction [12].

3.3 Non-isothermal analysis of the polymerisation of the epoxy-anhydride blend using DSC

The polymerisation of the unmodified epoxy/anhydride blend was also examined using dynamic DSC at various heating rates and the data (showing the onset/completion of reaction and the polymerisation enthalpy) are shown in Fig. 5, along with conversion data. A rescan was performed in each case to determine whether any residual exotherm as present in each case, but none was observed.

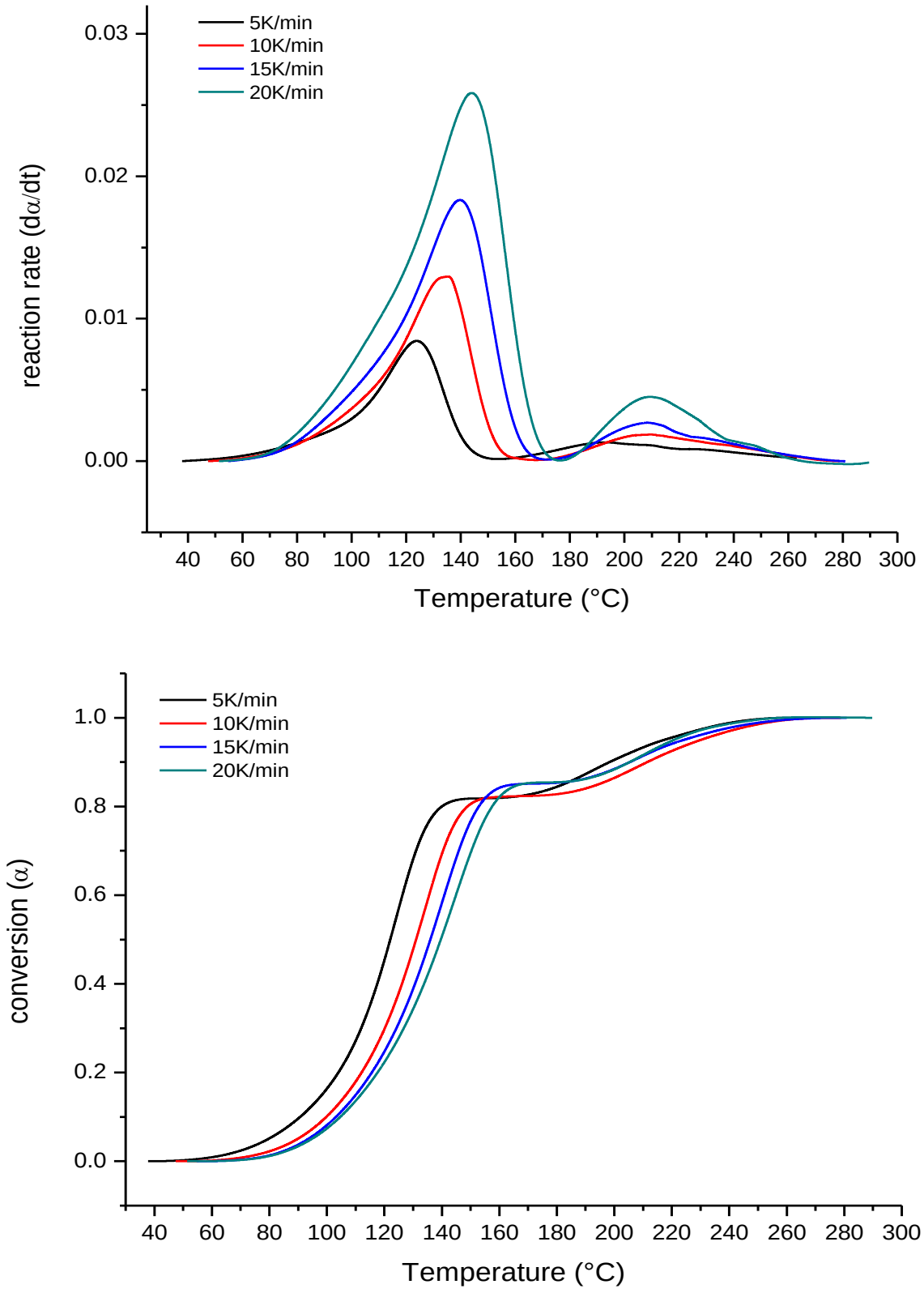

Fig. 5. Reaction rates (top) and fractional conversion (bottom) of the neat epoxy/anhydride (sample **1**) as a function of time at various heating rates

The plot of the reaction rate against temperature (Fig. 5, top) displays two discrete exothermic peaks due to the aforementioned etherification and esterification reaction, with the lower temperature cure peak assigned to the esterification reaction between the epoxy group and the anhydride; the higher temperature cure peak is attributed to the etherification reaction between epoxy groups based on previous work reported by Park and Lee [8]. The enthalpy for the lower esterification reaction is expressed in terms of kJ/mol of epoxy based on the EEW of 175.5 (Table 3)

Table 3

DSC scanning data for epoxy-anhydride (sample **1**) blend at various heating rates.

Heating rate (K/min)	**$T1_{onset}$ (°C)**	**$T1_{max}$ (°C)**	**ΔH_1**		**$T2_{onset}$ (°C)**	**$T2_{max}$ (°C)**	**ΔH_2**		**ΔH_p**	
			(J/g)	**(kJ/mol)**			**(J/g)**	**(kJ/mol)**	**(J/g)**	**(kJ/mol epoxy)**
5	**37.3**	127.9	234.7	41.2	155.3	192.4	46.7	8.2	281.4	49.4
10	**46.5**	140.5	221.4	38.9	167.6	209.9	50.6	8.9	272.0	47.7
15	**53.6**	147.9	216.1	37.9	173.1	207.0	41.5	7.3	257.6	45.2
20	**73.0**	153.1	211.2	37.1	177.3	210.2	47.6	8.4	258.8	45.4

Key

T_{onset} = the temperature at which the polymerisation reaction commences.

T_{max} = the temperature representing the maximum intensity of the polymerisation reaction (*N.B.* $T1_{max}$ indicates the peak maximum for the lower temperature reaction and ΔH_1 the corresponding reaction enthalpy).

ΔH_p = Total enthalpy of the polymerisation reaction(s).

Attempts were made to verify the chemical changes taking place using Raman spectroscopy, but the darkening colour of the resulting mixture (with increasing fluorescence) rendered this technique unfeasible. The esterification stage is a kinetically controlled process and most of the anhydride groups are consumed by reaction with the epoxies, but as the reaction proceeds, it becomes increasingly diffusion controlled, while etherification. Park and Lee reported [8] that the cure profile of an epoxy-rich system of DGEBA and hexahydropthalic anhydride under the influence of an imidazole catalyst also exhibited multiple peaks, which were also assigned in a

similar fashion. Fortunately, the dynamic DSC experiments yielded two discrete exotherms, which were analysed independently to give Arrhenius parameters for each process.

Once again, a number of approaches have been taken to the use of dynamic thermal data to generate kinetic information in thermosetting polymers and this was reviewed extensively in the context of epoxy resins by Barton [9]. Of these approaches, the Kissinger method [13] relates the peak maxium temperature, T_{max}, obtained using dynamic DSC and the activation energy (E_a) for data obtained at different heating rates (Fig. 5) (Eq. 8).

$$d \ln \varphi / d(1/T_{max}) = -(E_a/R) - 2.T_{max} \quad \text{(Eq. 8)}$$

(where φ = heat flow, T_{max} = polymerisation peak maximum from DSC, E_a = activiation energy, R = gas constant (8.314 J/mol.K).

However, (Eq. 8) is only really valid for first order reactions (n = 1) and as the polymerisation is more complex, a more general relationship at the peak maximum is

$$E/n = RT_{max}^2.r_{max} / \varphi (1-\alpha_{max}) \quad \text{(Eq. 9)}$$

(where r_{max} = rate of reaction at the peak maximum derived from DSC and α_{max} = conversion at the peak maximum)

In this way, the kinetics of the polymerisations were investigated using dynamic DSC at a variety of heating rates from which an activation energy of 70-80 kJ mol^{-1} was calculated using the Kissinger method, which correlated well with literature values for other epoxy-anhydride systems using the same treatment [14,15,16]. The kinetics were also determined using the Ozawa equation [17] which can be derived by integrating the basic kinetic equation for the special case of non-isothermal experiments in which samples were heated at a constant heating rate: = dT/dt (as in this case). As the series of experiments were performed at heating rates of 5, 10, 15, and 20 K/min., the T_{max} values were noted and a plot of $\ln(\beta)$- $1/T_{max}$ yielded straight lines with the slopes:

$log\beta = -0.4567(E_a/R).(1/T_{max})$ (Eq. 10)

(where β = heating rate, T_{max} = polymerisation peak maximum from DSC, E_a = activiation energy).

Thus, an activation energy of 89 kJ mol^{-1} was calculated using the non-isothermal isoconversional kinetic Ozawa method [18]. The Kissinger and Ozawa results are summarized in Table 4.

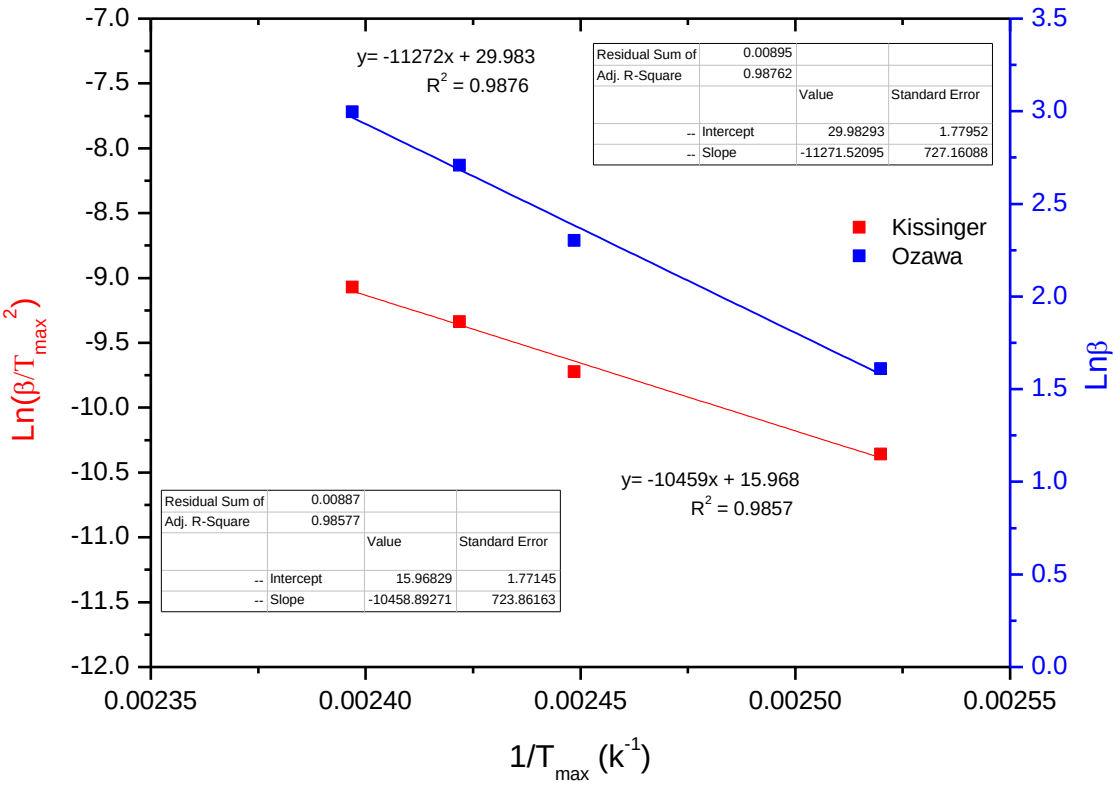

Fig. 6. Kinetic analysis using the Ozawa and Kissinger methods from scanning DSC data for the unmodified epoxy-anhydride blend (sample **1**), where β = heating rate.

Table 4

A comparison of the kinetic parameters for the epoxy-anhydride cure reaction using different models.

E_a of 1st reaction (kJ/mol)	**E_a of 2nd reaction (kJ/mol)**	**Pre-exponential factor at 393K (s^{-1})**	**K (s^{-1})**

Ozawa	Kissinger	Ozawa	Kissinger	1st reaction	2nd reaction	1st reaction	2nd reaction
89.09	86.96	123.8	122.3	9.00×10^{10}	1.38×10^{13}	0.249	0.0007

Whilst there have been many studies detailing the cure kinetics of epoxy-amine systems, including those involving POSS. Only comparatively recently have there been publications on the preparation of epoxy-POSS networks using carboxylic acid anhydride as the curing agent [19,20]. A formal kinetic analysis of the blends containing the mono-epoxy POSS is not presented since, strictly, the unmodified blend and the nano-reinforced blends do not share a thermal history. The essential pre-reaction step (to facilitate dispersion of the POSS) leads to ring opening and the esterification reaction, reducing the number of available active sites and reducing the measured exotherm.

3.4 Thermo-mechanical characterisation of the cured network

The DMTA data are presented in Fig. 7 and representative storage and loss modulus curves for sample **1** containing the DGEBA when cured with the anhydride are shown. Dynamic DSC was also used to corroborate the value of T_g and the epoxy-EP0402 samples were subjected to thermal analysis, measuring the heat flow of the material over a temperature range from 20 °C to 250 °C to obtain a glass transition temperature (Supplementary Material, S1-S3). During the first heat of the DSC scan there is some melting apparent at 50-90 °C and again at higher temperatures; these melting phases may be attributed to a presence of two phases or incomplete curing. The DSC thermogram of EP0402 (Supplementary, S2) exhibits melting transitions at 40-60 °C, 120 °C and 160 °C. The second melting phase of the epoxy-EP0402 resins at around 120 °C may be attributed to the melting of unreacted POSS. The DSC scan of the second heat however, shows a single transition indicating homogeneity in the samples. The T_g is also determined from the transition in the second heat and the data are also summarised in Table 5, as a function of EP0402 concentration in the anhydride system. The rescan data demonstrate that the range over which the transition is detected (135-155 °C) compares well with the loss modulus curve in Fig. 7 (tan δ invariably yields an inflated value for the magnitude of T_g).

The glass transition (α-transition) is clearly visible in the loss modulus data with a drop in the storage modulus of around 2400 MPa in this region (T_{max} = 138 °C in the loss modulus at 10 K/min); a subtle lower temperature transition (T_g') is visible between 50-100 °C. Each analysis

was performed several times and the peak maximum was found to be consistent (± 7 K). The breadth of the tan δ peaks can also indicate differences in the damping behaviour of cured epoxy resins (and other thermosets) and the peak width represents the temperature range over which the glass transition temperature occurs. Thus, a broad tan δ peak can be attributed to more heterogeneous networks containing both highly- and less-densely crosslinked regions [21]. This, in turn, results in a broad distribution of molecular mobilities or relaxation times. In this case, the data show a comparatively narrow distribution indicating a more homogeneous network. The addition of EP0402 POSS into the epoxy-anhydride system can increase the T_g with 2 wt-% EP0402 (sample **4**) exhibiting a T_g of 158 °C measured from the T_{max} in the loss modulus data). This is further supported from the storage modulus data (Fig. 7), where the sample containing 4 wt-% EP0402 displays a ~15 % decrease in storage modulus when compared with the neat resin (sample **1**). It is apparent from the storage modulus data that both samples containing 0.5 wt % and 1 wt % EP0402 are undercured using this cure regime, while the corresponding 2 wt % sample develops its maximum properties.

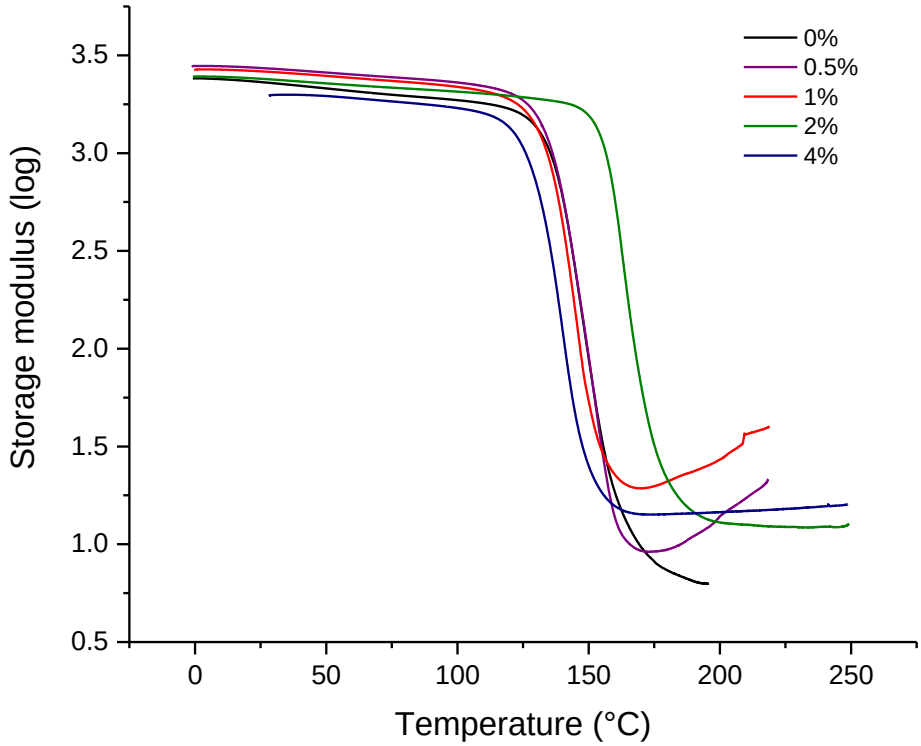

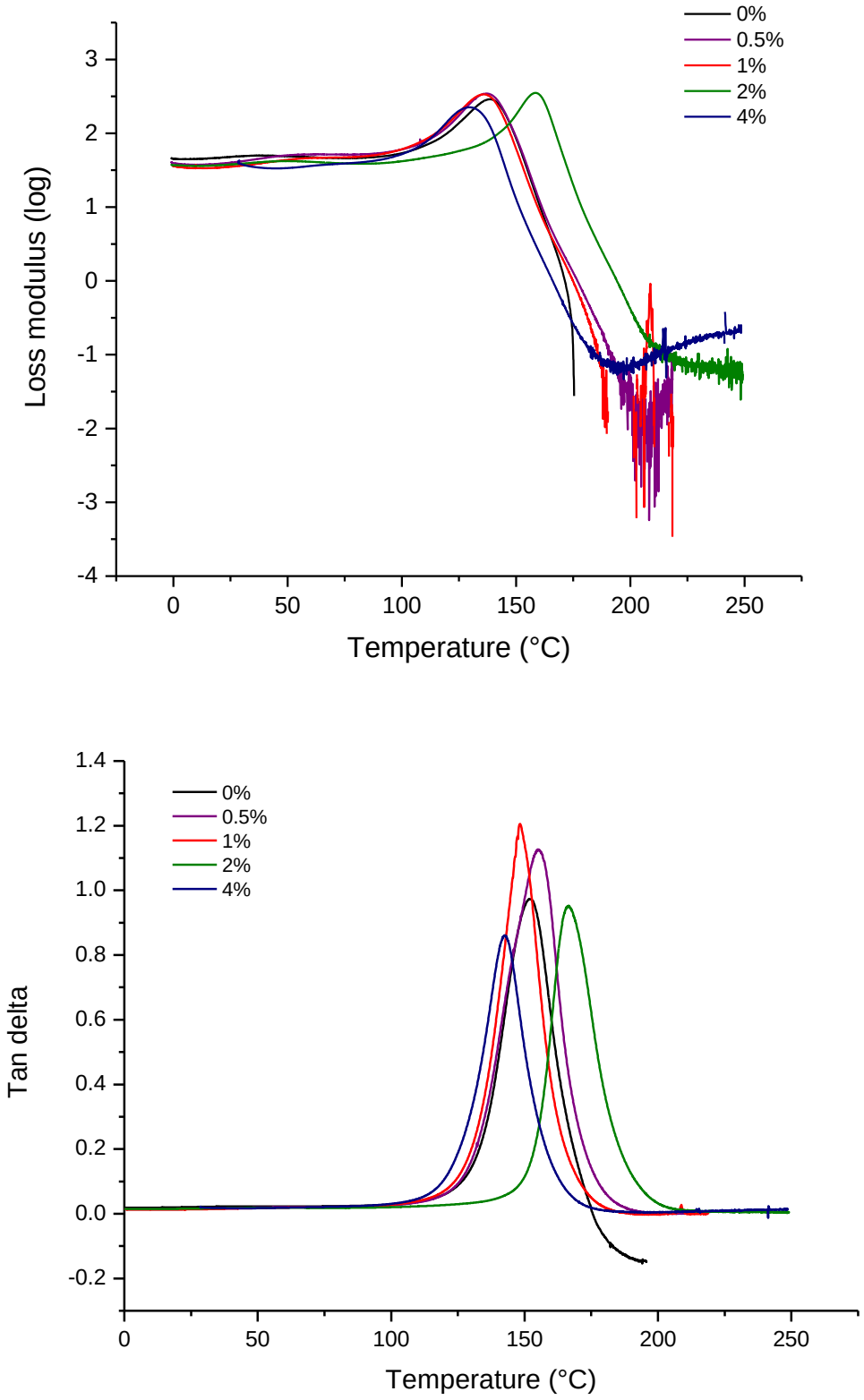

Fig. 7. Plots of $\log_{10}$ storage modulus (top), $\log_{10}$ loss modulus (middle) and tan δ (bottom) data for various epoxy-EP0402 samples (designated by the POSS content) as a function of temperature.

Table 5 summarises the T_g values (reported as the peak maxima from the loss modulus trace) obtained for the DMTA experiments (Fig. 7) and as a range from the DSC data; no clear trend in T_g is discernible based on the rule of mixtures as the mono-epoxy POSS is added. The loss modulus is revealed as single peak indicating the homogeneity of the samples. Thus, at the lowest levels of incorporation of EP0402 (0.5 and 1 wt-%) there is little effect on the observed T_g; at the highest level of incorporation (4 wt-%), T_g drops slightly; the epoxy containing 2 wt-% EP0402 (sample **4**) in singular in producing a significant increase in the observed T_g. Thus, there appear be two competing factors that are determining the glass transition temperatures: bulky POSS cages hinder polymer chain motion and therefore increase T_g, although the addition of POSS may also increase the free volume and thus result in a reduction in T_g.

Table 5

Glass transition temperatures for epoxy-EP0402 samples determined from different techniques.

Sample	**EP0402 content (weight %)**	**DMTA, Loss modulus (°C)**	**DSC (°C)**
1	**0**	138	123-163
2	**0.5**	137	124-139
3	**1**	135	119-137
4	**2**	158	136-154
5	**4**	129	123-126

The storage modulus generally appears to increase when the mono-epoxy POSS is added (Fig. 7), although the sample containing 4 wt-% EP0402 yields a lower storage modulus than the neat epoxy resin. The improvement in the dynamic storage moduli could be attributed to the nanoscale dispersion of POSS cages in the epoxy matrix.

As the addition of POSS generally increases the storage modulus and cross-link density (Fig. 7), indicating the covalently bound POSS cages within the epoxy matrix could be the dominant factor that affects the modulus. The unmodified epoxy blend (sample **1**) contains two difunctional reactants (DGEBA and a dicarboxylic acid, following ring opening of the cyclic anhydride) yielding a highly crosslinked network. Being a mono-epoxide, the addition of POSS forms a linear chain in the base catatalyzed reaction with anhydride, with the DGEBA serving as

a crosslinking agent. Consequently, the increasing addition of POSS (EP0402) should lead to a reduction in the crosslink density of the epoxy-anhydride network due to its low functionality. The crosslink density (ν) for each of the cured epoxy networks was calculated from the DMTA data using (Eq. 11) [22]:

$$\nu = G_e/\varphi R T_e \qquad \text{(Eq. 11)}$$

Where φ is taken as unity, G_e is the storage modulus strictly from a sample at equilibrium, but is taken at T_e, where $T_e = (T_g + 50\,K)$.

This equation is technically most appropriate for lightly cross-linked materials so it should only be used as a comparison between similar materials (*i.e.* in a homologous series), rather than giving a definitive value for crosslink density. This leads to a value of $\nu = 1.69$ mol m^{-3}, which compares well with $\nu = 1.7$ mol m^{-3} for a cured epoxy produced from difunctional monomers [23]. The calculated values of the cross-link density are shown in Table 6 suggests that only a small amount of EP0402 is required to increase the cross-link density of the matrix. The incorporation of POSS can lead to both an increase and decrease in T_g which can in turn have an effect on the cross-link density. The POSS units can act as either reinforcing fillers or as plasticising agents, depending on several competing factors such as restricting polymer chain movement and increasing free volume. As a result, no direct relationship between the cross-link density and T_g was observed, but a high value of T_g was consistently observed for the blend containing 2 wt-% POSS.

Table 6

Average cross-link density (ν, $\times 10^{-3}$ mol cm^{-3}) of epoxy-anhydride as a function of EP0402 content determined from DMTA data.

Sample	**EP0402 content (weight %)**	**T_e (K)**	**G_e (MPa)**	***ν*** **(x 10^{-3} mol cm^{-3})**
1	**0**	461	6.46	1.69 ± 0.8
2	**0.5**	460	17.3	4.52 ± 0.6
3	**1**	458	17.3	4.54 ± 0.5
4	**2**	481	12.6	3.51 ± 0.8

5	**4**	452	14.2	3.39 ± 0.6

The enhancement of rubbery modulus seen in similar nanocomposites has been attributed to the POSS filler effect [24], which includes (i) the hydrodynamic effect leading to strain amplification due to the presence of a hard filler in rubbery matrix, (ii) the formation of physical crosslinks – *i.e.* crystalline POSS domains (as the butyl-substituted POSS would be partly crystalline in the matrix) that are covalently attached to a network, (iii) the immobilization of network chains by interaction and formation of a hard interphase layer thus increasing both T_g and rubbery modulus, (iv) the percolation of the filler within a matrix. However, it is important to note that the levels of monoepoxy POSS incorporation are quite modest (< 4 wt-%) making (i) less significant; that the POSS is well dispersed making (ii) of less significance; that being covalently bonded, the percolation of POSS through the matrix (iv) is severely limited.

3.5 Examination of the thermal stability of the cured epoxy resin

Thermogravimetric analysis (TGA) was applied to evaluate the thermal stability of the cured epoxy-EP0402 resins. A series of TGA curves under nitrogen atmosphere for neat epoxy and epoxy-EP0402 performed at a ramp rate of 10 K/min is shown in Fig. 8. The thermal decomposition temperature (T_{dec}) of neat epoxy was not significantly affected by the addition of EP0402. Details of the changes in the T_{dec} and thermal residue are summarised in Table 7.

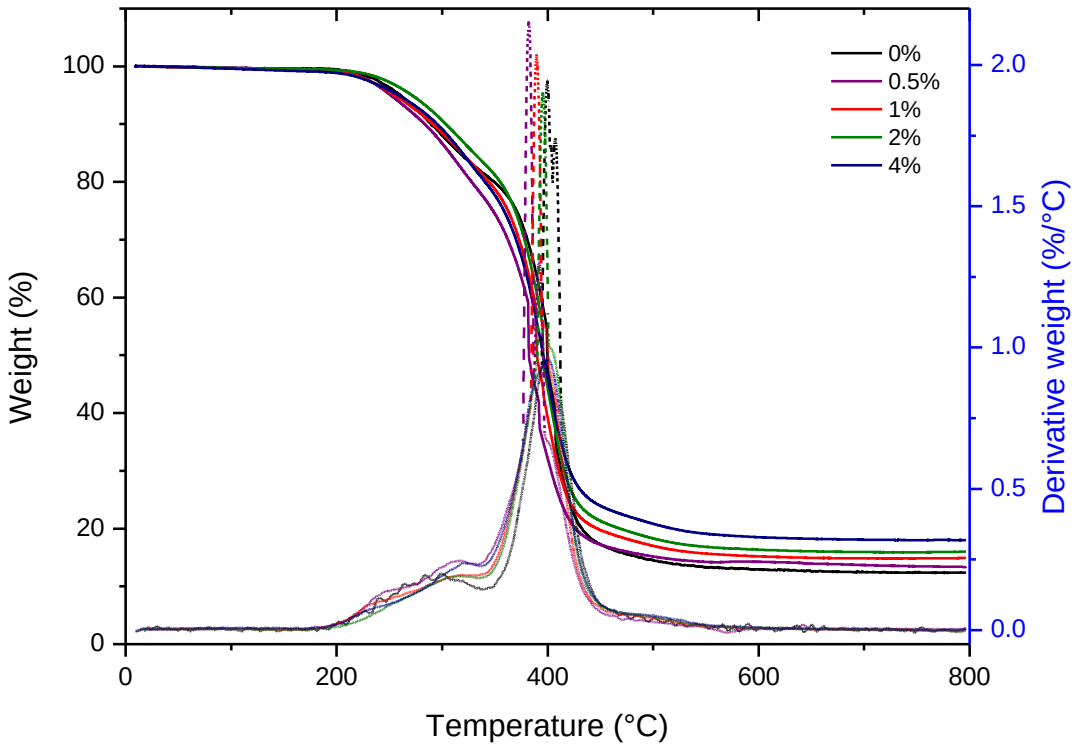

Fig. 8. TGA of epoxy-EP0402 samples.

Table 7

Thermal degradation temperature (T_{dec}) and thermal residue of epoxy-EP0402 samples**.**

EP0402 content (weight %)	Mass loss as a function of temperature (°C)				T_{dec} (°C)		Y_c (%)
	5%	10%	25%	50%	1st	2nd	
0	259.3	288.6	316.9	399.6	293.5	399.5	12.4
0.5	247.0	280.1	305.1	382.6	314.6	382.4	13.4
1	251.9	287.4	318.1	389.9	315.6	389.5	14.9
2	266.3	301.9	329.4	395.2	318.4	395.2	16.0
4	256.7	290.6	318.1	395.6	318.4	400.5	18.0

The TGA curves display similar degradation profiles indicating that the presence of POSS does not significantly alter the degradation mechanism of the epoxy matrix (at this level of incorporation), although there is some variation in the peak maxima denoting the maximum rate of mass loss. The degradation process is composed of three steps with the initial decomposition approximating to 250-300 °C with loss of almost 20 % of the mass of the sample. The first step may be attributed to the loss of unreacted epoxy, or impurities in the matrix and breakdown of inter-ring bridges. This is not dissimilar from recent research published by us in the area of polybenzoxazine resins [25], which form similar network structures of comparable stability. The second and third stages of degradation occur at around 400 °C and 450 °C for the neat resin and slightly lower for 0.5, 1 and 2 wt-% EP0402, caused by thermal degradation of the cured network and polymer chain backbone. Decomposition may involve other processes such as dehydration of secondary hydroxyl groups followed by formation of free radicals. The degradation process is a complex process, which involves a variety of reactions such as cross-linking, branching, recombination, rearrangement *etc*. Recombination of free radicals results in a highly thermally stable char. The addition of POSS appears to bring down the T_{dec} initially;

however, as the concentration of EP0402 increases, the T_{dec} begins to increase. As expected, the char yields increase with the POSS content, due to the formation of an inert silica layer on the surface of materials when decomposition takes place [26,27,28]. The pre-reacted system is assumed to have formed covalent bonds with the epoxy-anhydride system, which may also contribute to the enhancement of the initial decomposition temperature.

3.6 Determination of moisture absorption

The unmodified cured epoxy samples were exposed to atmospheres of different controlled humidities and the weight gain curves are presented as a function of square root time in Fig. 9. The two main characteristics of Fickian behaviour are that: (1) the absorption curve should be linear and (2) the moisture content should reach saturation level after a time period. All samples show an almost linear relationship between the moisture uptake and the square root of time at the beginning of the absorption process. The water concentration gradient is therefore the driving force that leads to water absorption in epoxy systems. The values for equilibrium mass uptake (M_m) and diffusivity (D) are listed in Table 8 and it can be seen that the diffusion coefficient changed when EP0402 was incorporated into the epoxy-anhydride system. An increase in diffusion coefficient may be attributed to an increase in free volume, but this does not appear to be related directly to increasing EP0402 content.

Table 8

Maximum water absorption and diffusivity of epoxy-EP0402 resins at various humidities.

RH (%)	**EP0402 content (weight %)**	**Thickness (mm)**	**M_m (%)**	**Diffusivity (x 10^{-5} mm^2/sec)**
33	**0**	3.48	0.60	2.1
	0.5	3.08	0.54	2.6
	1	3.03	0.52	3.1
	2	2.85	0.54	2.6
	4	2.66	0.64	2.0
52	**0**	3.06	1.83	1.3
	0.5	2.95	1.42	2.2

	1	3.10	1.41	2.6
	2	2.95	1.45	2.0
	4	2.66	1.47	1.7
75	**0**	3.05	1.83	1.4
	0.5	3.08	1.41	2.7
	1	3.16	1.35	2.6
	2	2.94	1.39	2.3
	4	2.79	1.59	1.6

Key

M_m = Equilibrium mass uptake

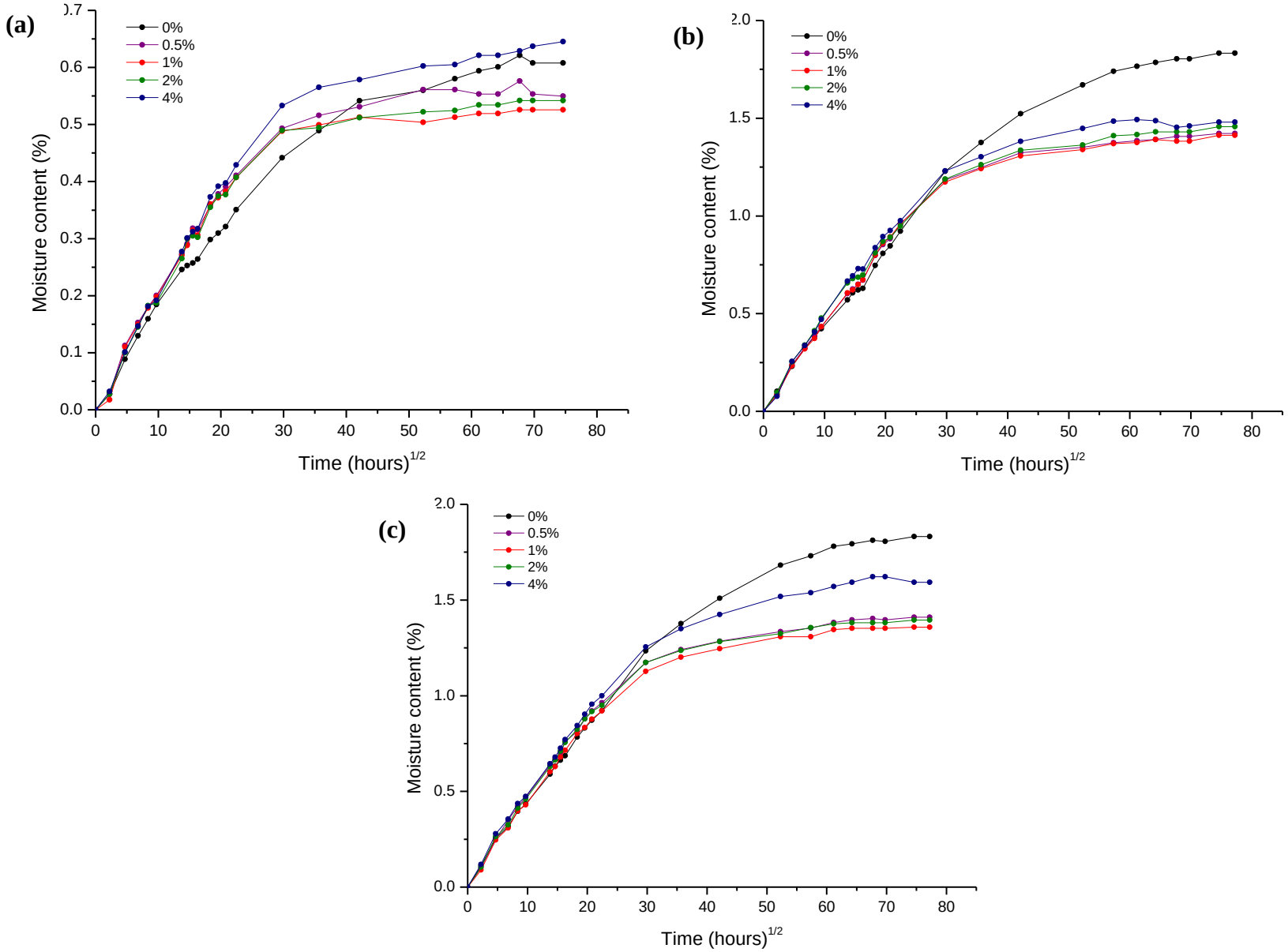

Fig. 9. Water absorption graphs for epoxy-EP0402 samples containing different concentrations of EP0402 at (a) 33 % RH (b) 52 % RH and (c) 75 % RH.

DMTA analysis was performed on each sample after ~6000 hours in the various humidity chambers and Table 9 summarises the T_g and cross-link density before and after moisture testing. There is very little change in the cross-link density of the samples after moisture testing with most samples experiencing a small decrease (*e.g.* the T_g of the neat resin experiences a drop of *ca.* 20 K for 33 % RH with a maximum moisture uptake of 0.60 %). Epoxy resins are well known for their ability to sorb moisture showing typical moisture uptake of the order of *ca.* 4-7 % (in non speciality polymers that have not been modified to reduce moisture uptake). Furthermore, Wright established a semi-empirical guide to demonstrate that an average reduction in T_g of up to 20 K was observed for every 1% of moisture sorbed [29]. The unmodified epoxy structure featured in this study is routinely employed in advanced composites due to its reduced moisture uptake. As the manufacture of a large component might take months or even several years to complete (and total elimination of moisture from the production environment would be impractical), there is much time available for the sorption of moisture to reach equilibrium. With the addition of POSS, the maximum moisture uptake is reduced to 0.52-0.54 % for 0.5, 1 and 2 % POSS content. This reduction in the moisture absorption is accompanied by a T_g value that remains largely unaffected, unlike the neat resin, which indicates that the addition of EP0402 reduces the plasticising affect in epoxy-anhydride systems.

Table 9

A comparison of the T_g and cross-link density of epoxy-EP0402 resins before and after moisture testing.

RH (%)	**EP0402 content (weight %)**	**Loss modulus (°C)**		**Decrease in T_g (°C)**	**M_m (%)**	***v*** **(x 10^{-3} mol cm^{-3})**	
		Before	**After**			**Before**	**After**
33	**0**	138.6	118.9	19.7	0.60	1.9	2.4
	0.5	153.3	149.8	3.5	0.54	3.2	2.8
	1	148.3	145.9	2.4	0.52	5.2	3.7
	2	158.5	148.8	9.7	0.54	3.2	3.0
	4	129.6	121.3	8.3	0.64	3.9	3.1
52	**0**	138.6	102.1	36.5	1.83	1.9	1.6
	0.5	153.3	136.7	16.6	1.42	3.2	2.9

	1	148.3	135.8	12.5	1.41	5.2	2.9
	2	158.5	140.9	17.6	1.45	3.2	3.5
	4	129.6	125.8	3.8	1.47	3.9	2.1
75	**0**	138.6	107.0	31.6	1.83	1.9	2.3
	0.5	153.3	141.2	12.1	1.41	3.2	3.1
	1	148.3	138.9	9.4	1.35	5.2	3.2
	2	158.5	144.5	14.0	1.39	3.2	2.6
	4	129.6	121.2	8.4	1.59	3.9	2.1

Key

M_m = Equilibrium mass uptake

v = Crosslink density calculated from DMTA data

The effects on the tan δ response of the samples after exposure to moisture are shown in Fig. 11. The overall reduction in the tan δ values and the shift of T_g to lower temperatures indicates that the sorbed water acts as a plasticiser, increasing chain mobility. The hydrated samples also show a splitting of the tan δ peaks which may be attributed to the presence of two types of bound water: singly- and doubly-hydrogen bonded. Single hydrogen bonded water can disturb the inter-chain van der Waals forces in the polymer network resulting in an increase in chain mobility which is known as plasticisation; double hydrogen bonds form with the polymer network due to prolonged exposure and can act as cross-links in between polymer chains. Therefore, the desorption of water during DMTA testing can lead to two peaks, since type 1 bound water can dissipate from the matrix first due to lower activation energy, leaving type 2 bound water which requires higher temperatures for desorption.

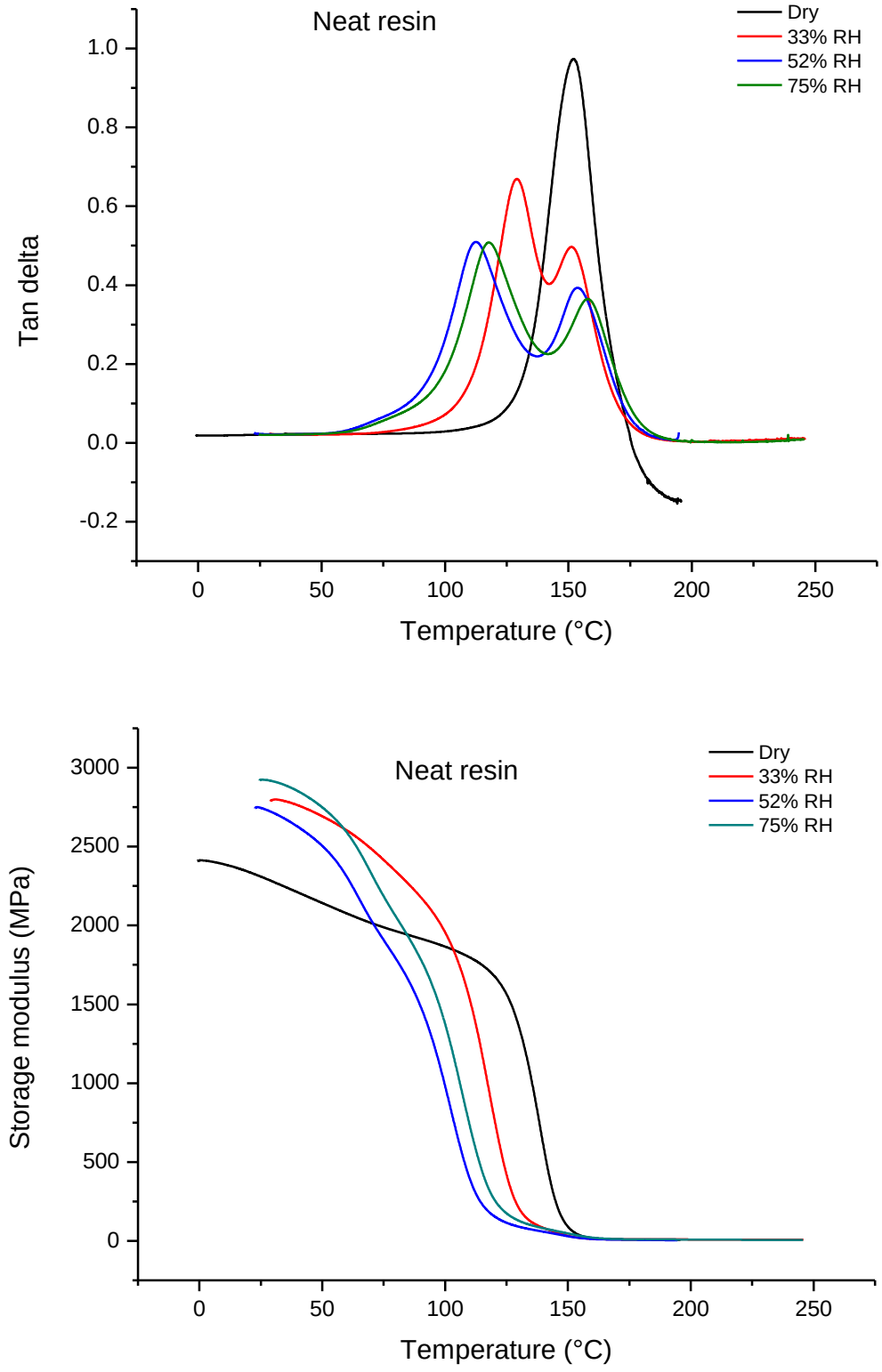

Fig. 10. Storage modulus (top) Tan δ (bottom) *vs.* temperature of the neat resin (0 % EP0402) at various humidities.

Fig. 10 also shows the storage modulus as a function of temperature of the neat resin after moisture testing for the various humidity environments. The storage modulus at room

temperature increased by ~28 % after exposure to moisture. This increase may be attributed to hydrogen bonding between water molecules and excess anhydride or epoxy groups. However, as the temperature increases the storage modulus declines quickly when compared to the 'dry' sample. A change in the initial β-transitions can also be observed: for the 'dry' sample, the β-transitions occur between 30-90 °C, whereas the hydrated samples show a β-transition between 65-95 °C.

Fig 11 and 12 show the tan δ traces and storage modulus for the 'dry' and 'wet' samples for each POSS loading respectively. A decrease in the peak of tan δ and a shift to lower temperatures of the glass transition region with increasing water content is observed. This reflects the plasticising effect of water on the polymer matrix. The broadening of secondary tan δ peaks in the glass transition region followed a different trend for each POSS loading. At the lower POSS content (0.5 wt % and 1 wt %) there are two peaks for 52 % and 75 % RH. This is also observed for the neat resin indicating that they behave in a similar manner. However, for 2 and 4 wt-% loadings the double peaks are not observed indicating that the introduction of POSS at these levels reduces the plasticising effect. For 0.5 and 1 wt-% POSS addition the storage modulus decreases after moisture testing, however, for 2 and 4 wt-% addition, the storage modulus is higher than the unmodified resin at the lower temperatures which may be attributed to the toughening of the epoxy matrix from the type 1 bound water molecules.

It has been observed [30] that in some instances POSS bearing aliphatic substituents have migrated to the sample surface of polymer blends and dramatically increase the hydrophobicity of the nanocomposites. However, the pre-reaction of the POSS with one component of the blend prior to incorporation makes it less likely that the POSS is drawn to the surface of the resin, since its mobility will be severely restricted. Rather, the POSS becomes well dispersed within the three-dimensional network. This situation is not dissimilar from recent research published by us in the area of POSS nano-reinforced polypropylene matrices [5] in which the dispersion of the POSS (at similar levels of loading, *ca.* 5 wt-%) was confirmed using SEM-EDX. The authors believe that the flexibility of the alkylene tether, by which the POSS is bonded covalently, allows sufficient movement to enable molecular cavities to be 'filled' by the hydrophobic POSS cage, thus shielding potential sites for hydrogen bonding. This view is supported by molecular modelling studies undertaken on matrices containing similar epoxy/diamine/POSS compositions [3], but not presented in this manuscript.

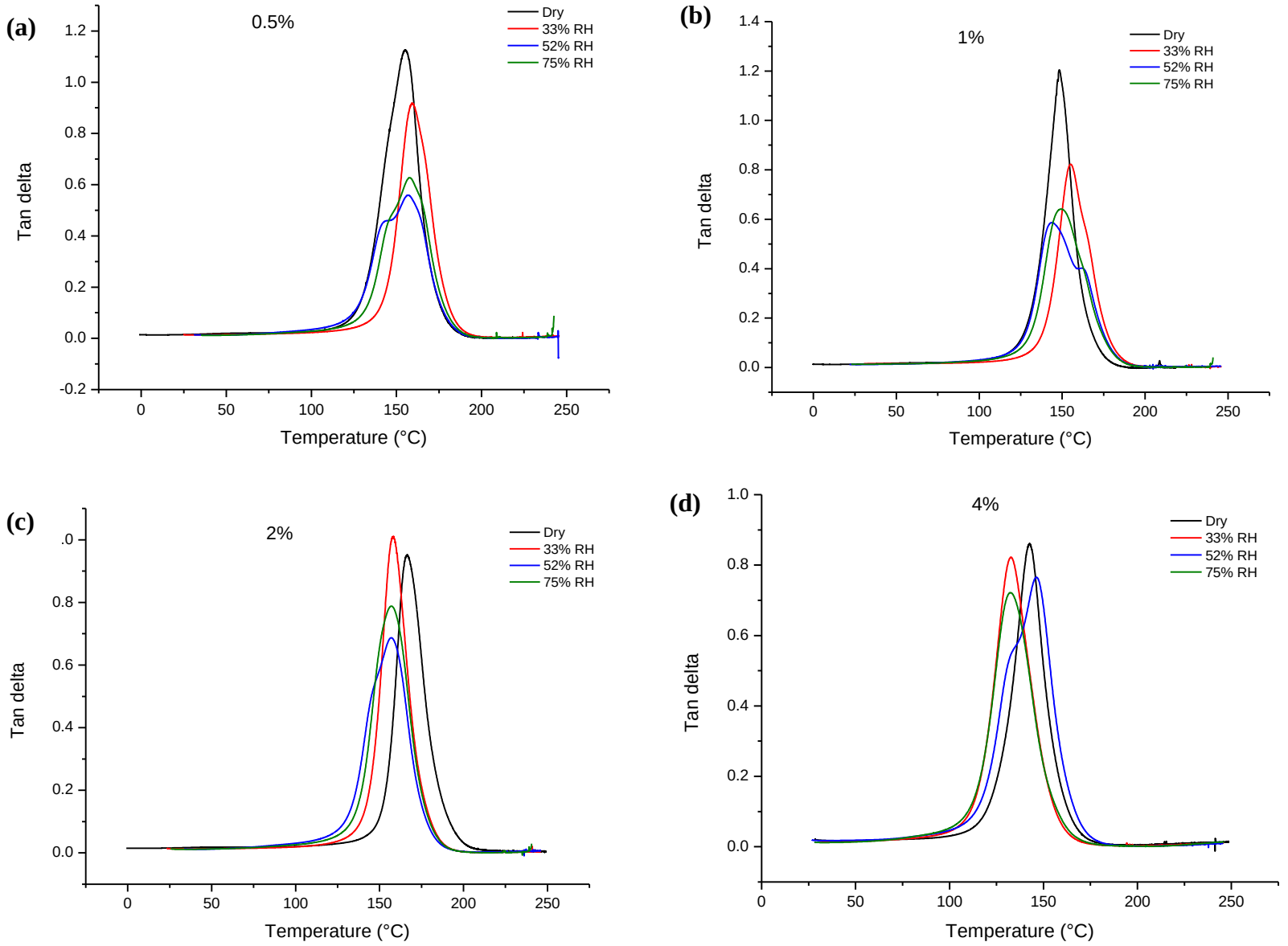

Fig. 11. Changes in tan δ as a function of temperature at varying humidities of **(a)** 0.5 % **(b)** 1 % **(c)** 2 % and **(d)** 4 % epoxy-EP0402 samples.

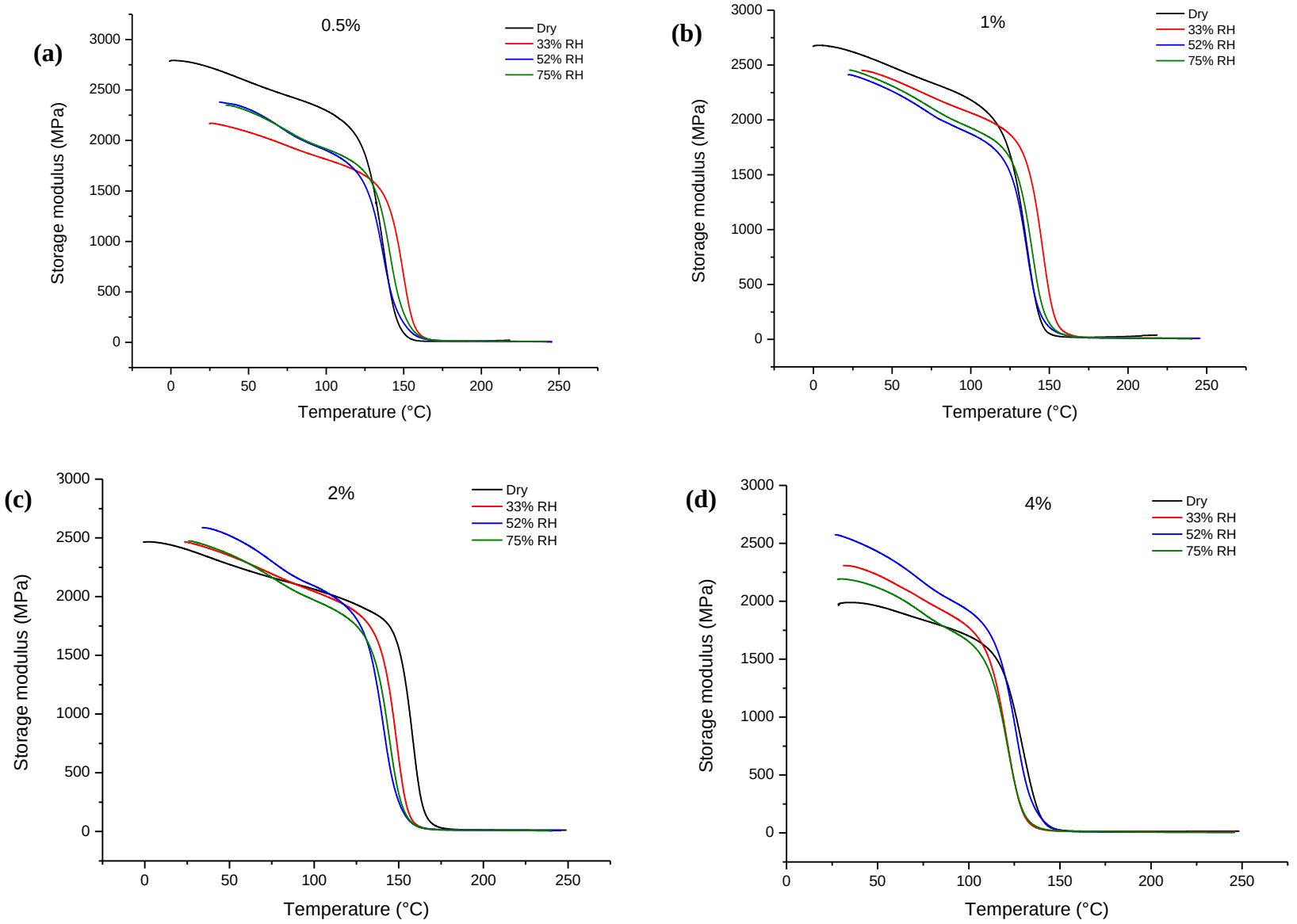

Fig. 12. Changes in storage modulus as a function of temperature at varying humidities of **(a)** 0.5 % **(b)** 1 % **(c)** 2 % and **(d)** 4 % epoxy-EP0402 samples.

4. Conclusions

The effect of a mono-functional POSS on the viscoelastic properties in an epoxy-anhydride system has been investigated. Two reaction mechanisms were observed and attributed to esterification at the lower temperatures and etherification at temperatures above 180 °C. Using the Ozawa and Kissinger method, the activation energy was found to be between 70-80 kJ/mol, which is consistent with other epoxy-anhydride systems. From the thermo-mechanical analysis, the incorporation of POSS into the epoxy-anhydride network improved the T_g and increased cross-link density, indicating a more rigid network. However, the values did not display a trend based on the simple rule of mixtures, suggesting that the addition of POSS can also lower the T_g and cross-link density due to competing factors as previously described. The TGA data showed that the char yield increases with very little changes in the degradation temperature. Samples were subjected to various relative humidities to examine the effects of POSS on the moisture absorption in epoxy-anhydride system. The results showed that 1 wt-% EP0402 can reduce the moisture uptake by ~25 % at 75 % relative humidity. As a result, the T_g reduced by ~10 K, whereas the T_g for the neat resin reduced by ~31 K. These results show that the addition of POSS not only improves the thermo-mechanical properties but it can also reduce the moisture absorption with minimal effects on the T_g.

Acknowledgements

We thank EADS Astrium for financial support (WT, JVA) in the form of a studentship and Dr Thomas Stute (Astrium, Friedrichshafen, Germany), Dr John Houghton (Astrium, Stevenage, UK), Dr Bernard Gergonne (Astrium, Toulouse, France) for practical assistance and useful discussions during the production of this manuscript.

This paper is dedicated to the memory of the late Dr John Michael Barton (1935-2014).

References

[1] I. Hamerton, Epoxy resins, in Encyclopaedia of Chemical Processing, S. Lee (Ed.) DOI: 10.1081/E-ECHP-12000775, 2006, Taylor & Francis.

[2] Araldite LY566/Aradur 906/Accelerator DY070, Huntsman Advanced Materials http://mouldlife.co.uk/download/tds/Araldite%20LY%20556_Aradur%20906_Accelerator%20DY070_TDS.pdf (accessed 25 April 2014).

[3] I. Hamerton, W. Tang, J.V Anguita, S.R.P. Silva, React. Func. Polym. 74 (2013) 1-15.

[4] G. Li, L. Wang, H. Ni, C.U. Pittman, Jr., J. Inorg. Org. Polym. 11 (2001) 123-154.

[5] E.R. Smith, B.J. Howlin, I. Hamerton, J. Mater. Chem. A 1 (2013) 12971-12980.

[6] S. Nagendiran, M.K. Alagar, I. Hamerton, Acta Mater. 58 (2010) 3345-3356.

[7] M.A. Boyle, C.J. Martin, J.D. Neuner, Epoxy resins, In ASM Handbook Composites, ASM International (2001) p 195.

[8] W.H. Park, J.K. Lee, J. Appl. Polym. Sci. 67 (1998) 1101.

[9] J.M. Barton, Adv. Polym. Sci., K. Dusek (Ed.) volume 72, Springer-Verlag: Berlin (1985) p 111.

[10] S. Sourour, M. R. Kamal, Thermochim. Acta 14 (1976) 41.

[11] K. Horie, H. Hiura, M. Sawada, I. Mita, H. Kambe, J. Polym. Sci. Part A-1: Polym. Chem. 8 (1970) 1357.

[12] I. Hamerton, Recent Developments in Epoxy Resins, In Rapra Review Reports, R. Dolbey, Ed. RAPRA: Shropshire, 1996, Vol. 8.

[13] H. Kissinger, Anal. Chem. 21 (1957) 1702.

[14] P. Navabpour, A. Nesbitt, T. Mann, R.J. Day, J. Appl. Polym. Sci. 104 (2007) 2054.

[15] U. Khanna, M. Chanda, J. Appl. Polym. Sci. 50 (1993) 1635.

[16] Y. Liu, Z. Du, C. Zhang, C. Li, H. Li, J. Appl. Polym. Sci. 103 (2007) 2041.

[17] T. Ozawa, Anal. Chem. 2 (1970) 301-324.

[18] J.H. Flynn, J. Thermal Anal. Chem. 27 (1983) 95-102.

[19] J.K. Herman Teo, K.C. Teo, B. Pan, Y. Xiao, X. Lu, Polymer 48 (2007) 5671.

[20] F. Xiao, Y. Sun, Y. Xiu, C.P. Wong, J. Appl. Polym. Sci. 104 (2007) 2113.

[21] A.R. Kannurpatti, J.W. Anseth, C.N. Bowman, Polymer 39 (1998) 2507-2513.

[22] D.J. Allen, H. Ishida, J. Appl. Polym. Sci. 101 (2006) 2798 –2809.

[23] F. Cardona, C. Moscou, Synthesis and characterisation of modified phenolic resins for composites with enhanced mechanical properties, In: ACMSM 20: Futures in Mechanics of Structures and Materials, 2-5 Dec 2008, Toowoomba, Australia, 2009.

[24] N.T. Dintcheva, E. Morici, R. Arrigo, F.P. La Mantia, Polym. J. 46 (2014) 160-166.

[25] I. Hamerton, S. Thompson, B.J. Howlin, C.A. Stone, Macromolecules 46 (2013) 7605-7615.

[26] Z. Zhang, A. Gu, G. Liang, P. Ren, J. Xie, X. Wang, Polym. Degrad. Stab. 92 (2007) 1986.

[27] Z. Zhang, G. Liang, X. Wang, Polym. Bull. 58 (2007) 1013.

[28] H. Dodiuk, S. Kenig, I. Blinsky, A. Dotan, A. Buchman, Internat. J. Adhesion Adhesives 25 (2005) 211.

[29] W.W. Wright, Composites 37 (1981) 201-205.

[30] Y. Tang, M. Lewin, Polym. Adv. Technol. 20 (2009) 1-15.